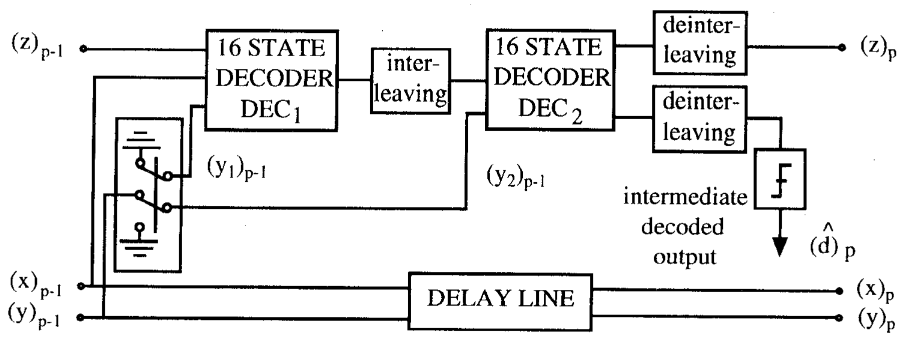

Fig. 8. Decoding module (level p).

With the feedback decoder, the LLR $\Lambda_1(d_k)$ generated by decoder DEC_1 is now equal to

$$\Lambda_1(d_k) = \frac{2}{\sigma^2} x_k + \frac{2}{\sigma_z^2} z_k + W_{1k} \tag{44}$$

where W_{1k} depends on sequence $\{z_n\}_{n \neq k}$. As indicated above, information z_k has been built by decoder DEC_2. Therefore z_k must not be used as input information for decoder DEC_2. Thus decoder DEC_2 input sequences will be sequences $\{\tilde{\Lambda}_1(d_n)\}$ and $\{y_{2k}\}$ with

$$\tilde{\Lambda}_1(d_n) = \Lambda_1(d_n)_{z_n=0}. \tag{45}$$

Finally, from (40), decoder DEC_2 extrinsic information $z_k = W_{2k}$ after deinterleaving can be written as

$$z_k = W_{2k} = \Lambda_2(d_k)|_{\tilde{\Lambda}_1(d_k)=0} \tag{46}$$

and the decision at the decoder DEC output is

$$\hat{d}_k = \mathrm{sign}[\Lambda_2(d_k)]. \tag{47}$$

The decoding delays introduced by the component decoders, the interleaver and the deinterleaver imply that the feedback piece of information z_k must be used through an iterative process.

The global decoder circuit is made up of P pipelined identical elementary decoders. The pth decoder DEC (Fig. 8) input, is made up of demodulator output sequences $(x)_p$ and $(y)_p$ through a delay line and of extrinsic information $(z)_p$ generated by the $(p-1)$th decoder DEC. Note that the variance σ_z^2 of $(z)_p$ and the variance of $\tilde{\Lambda}_1(d_k)$ must be estimated at each decoding step p.

For example, the variance σ_z^2 is estimated for each M^2 interleaving matrix by the following:

$$\sigma_z^2 = \frac{1}{M^2} \sum_{k=1}^{M^2} (|z_k| - m_z)^2 \tag{48a}$$

where m_z is equal to

$$m_z = \frac{1}{M^2} \sum_{k=1}^{M^2} |z_k|. \tag{48b}$$

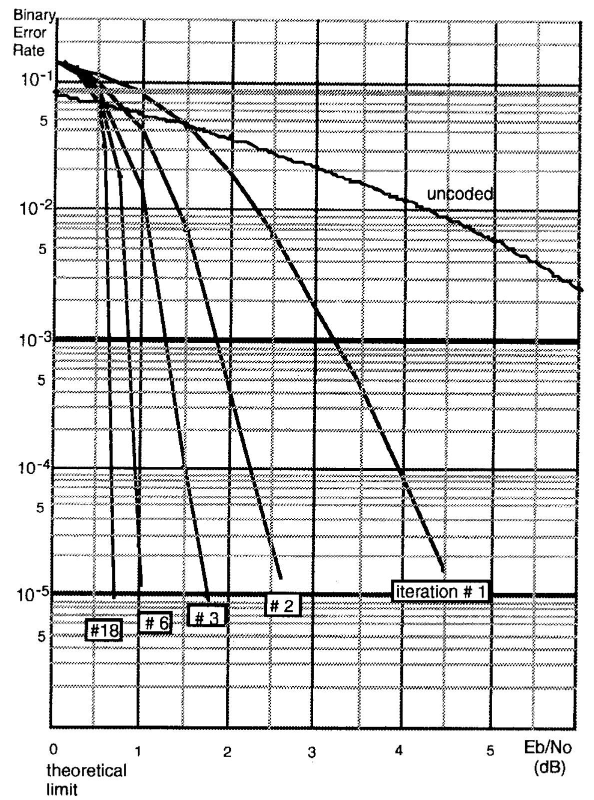

Fig. 9. BER given by iterative decoding ($p = 1, \cdots 18$) of a rate $R = 1/2$ encoder, memory $\nu = 4$, generators $G_1 = 37, G_2 = 21$, with interleaving 256×256.

B. Interleaving

The interleaver is made up of an $M \cdot M$ matrix and bits $\{d_k\}$ are written row by row and read following the nonuniform rule given in Section III-B2. This nonuniform reading procedure is able to spread the residual error blocks of rectangular form, that may set up in the interleaver located behind the first decoder DEC_1, and to give a large free distance to the concatenated (parallel) code.

For the simulations, a 256.256 matrix has ben used and from (19), the addresses of line i_r and column j_r for reading are the following:

$$i_r = 129(i + j) \qquad \mathrm{mod} \cdot 256$$

f the decoding trellis. Thus,
tial dependence of decoding
application of the Viterbi
since the branch complexity
ce more time to decode. This
eliminated using a technique

erbi algorithm by employing
it must be performed at each
used to do the operations in
2^ν operations serially. Thus,
s a factor of 2^ν advantage in
2^ν times as much hardware.
about 1/3 for a large subclass
compare–select–add (CSA)
ls of this *differential Viterbi*

sults illustrating the perfor-
Figure 12.17. The bit-error
odes with constraint lengths
as a function of the bit SNR
channel in Figure 12.17(a).
d-quantized ($Q = 2$) channel
mory was $\tau = 32$. Note that
of soft decisions (unquantized
2). This improvement is illus-
e of the optimum constraint
o (unquantized outputs) and
2.17(c) is the uncoded curve
es shows real coding gains of
dB in the quantized ($Q = 8$)
$= \infty$) soft-decision case at a
only about 0.2-dB difference
d the unquantized ($Q = \infty$)
h to gain by using more than
(d), the performance of this
and ∞ (no truncation) for a
itput. Note that in both cases
ance by about 1.25 dB, that
at $\tau = 32 = 8\nu$ performs the
1/2 codes.) The performance
engths $\nu = 3, 5$, and 7 listed
a continuous-output AWGN
than the corresponding rate
a 0.25 dB and 0.5 dB. This is
l d_{free} in decibels, is larger at

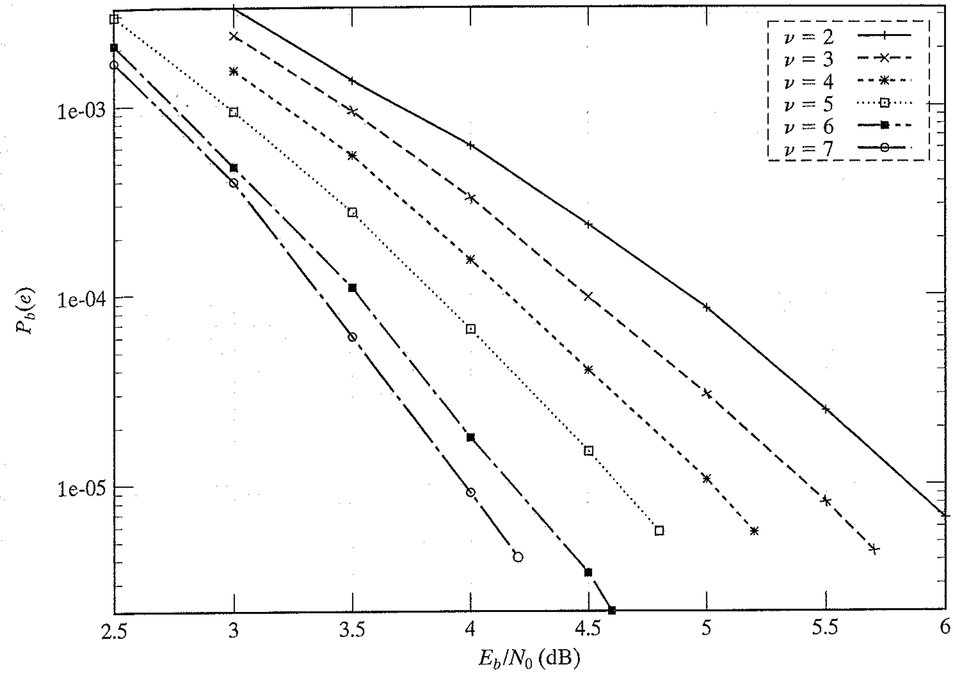

(a)

(b)

FIGURE 12.17: Simulation results for the Viterbi algorithm.